FDTD analysis of Talbot effect of a high density grating

Yunqing Lu (陆云清)[1,2], Changhe Zhou (周常河)[1], and Hongxin Luo (罗红心)[1]

[1] *Shanghai Institute of Optics and Fine Mechanics, Chinese Academy of Sciences, Shanghai 201800,*
[2] *Graduate of the Chinese Academy of Sciences, Beijing 100039*

Talbot effect of a grating with different flaws is analyzed with the finite-difference time-domain (FDTD) method. The FDTD method can show the exact near-field distribution of different flaws in a high-density grating, which is impossible to obtain with the conventional Fourier transform method. The numerical results indicate that if a grating is perfect, its Talbot imaging should also be perfect; if the grating is distorted, its Talbot imaging would also be distorted. Furthermore, we can evaluate high density gratings by detecting the near-field distribution.

OCIS codes: 070.6760, 110.6760, 050.1950, 260.2110.

When a periodic object is illuminated by a monochromatic light wave, an image of the object will appear at some distant planes behind the object, which is called Talbot effect[1]. Talbot effect has been extensively analyzed with the scale Fourier transform method. For a plane wave, the distance Z_n behind the object is given by $Z_n = nZ_t$, where $Z_t = 2d^2/\lambda$, λ is the wavelength of the incident light, d is the period of the grating, and n is a positive integer. The self-imaging of any type of gratings at Talbot distance can be explained by means of the Fresnel equation. It is also shown that at some fractional Talbot planes the diffracted intensity distribution is also similar to the object[2−4]. And there are simple relations, such as the symmetry principle and regularly rearranged-neighboring-phase-difference (RRNPD) rule[5].

The finite-difference time-domain (FDTD) method has been used extensively in calculating many electromagnetic problems since the initial work of Yee[6], and its popularity continues to grow as computing cost continues to decline. Nowadays, the FDTD method is one of the most popular numerical methods for the solution of electromagnetic problem[7]. It is also applied in optical waveguides[8], photonic crystal[9], and diffractive optical elements (DOEs)[10−12]. Ichikawa analyzed the diffraction gratings with feature sizes comparable to the wavelength with FDTD method[11]. The diffraction efficiencies were obtained and in good agreement with other commonly used numerical methods in the frequency domain. And the femtosecond-order optical pulses were applied in this diffraction problem too[12]. In this paper, Talbot effect of a grating with different flaws is analyzed with the FDTD method. To our knowledge, it is the first time that FDTD method is applied to analyzing the performance of this kind of diffraction. The flaws might be caused by the fabrication errors, such as the irregular flaws and stochastic fluctuation of the groove depth. For a grating with stochastic flaws, we cannot obtain the exact near-field distributions with the conventional Fourier transform method. It is necessary to use FDTD method for analysis of this kind of diffraction. The finite-difference time-domain method is a powerful method that can be used to analyze the diffraction in the near field when there is variation of the electromagnetic field distribution. We analyzed the Talbot effect with different kinds of flaws. We try to recognize the relation between the flaws and the near-field distributions; when there is no flaw, the Talbot imaging of a grating will be perfect. When the grating is distorted, the Talbot image must be distorted.

The FDTD algorithm used here is the most standard one based on the Yee lattice. In this paper we assume that the grating is normally illuminated by a TE plane wave. In such case, the solutions of Maxwell's curl equations in a finite-difference expression reduce to

$$E_z^{n+1}(i,k) = \frac{2\varepsilon(i,k) - \sigma(i,k)\Delta t}{2\varepsilon(i,k) + \sigma(i,k)\Delta t} E_z^n(i,k) + \frac{2\Delta t}{2\varepsilon(i,k) + \sigma(i,k)\Delta t} \times \left[\frac{H_y^{n+1}(i,k) - H_y^{n+1}(i,k-1)}{\Delta x}, - \frac{H_x^{n+1}(i,k) - H_x^{n+1}(i-1,k)}{\Delta y}\right], \quad (1)$$

$$H_y^{n+1}(i,k) = H_y^n(i,k) + \frac{\Delta t}{\mu(i,k)} \frac{E_z^n(i+1,k) - E_z^n(i,k)}{\Delta x}, \quad (2)$$

$$H_x^{n+1}(i,k) = H_x^n(i,k) + \frac{\Delta t}{\mu(i,k)} \frac{E_z^n(i,k+1) - E_z^n(i,k)}{\Delta y}, \quad (3)$$

here, ε, μ, and σ are permittivity, permeability, and the medium's electric conductivity, respectively. Δx, Δy, and Δt are lengths of the unit cell in the x and y directions and a single time step, respectively. We let $\Delta x = \Delta y = \lambda/20$ and $\Delta t = \Delta x/2c$ in the simulation. Integer values i and k denote the position of sample points in the x and y directions. For permittivity we use the expression $\varepsilon = \varepsilon_0 {\varepsilon_j}^{\mathrm{r}}$, where ε_0 is the value in a vacuum and ${\varepsilon_j}^r$ is the relative permittivity of the value of the jth medium. The propagation of the electromagnetic field is simulated with Eqs. (1)-(3), step by step in the time domain.

An example of the diffraction gratings used here is a dielectric grating with period of 2.6λ, and the peak-to-valley modulation depth of λ. The sine-shaped-surface-relief grating was assumed to be fabricated in glass (relative permittivity ${\varepsilon_1}^{\mathrm{r}} = 2.25$) and the outside medium is air (relative permittivity ${\varepsilon_2}^{\mathrm{r}} = 1.0$). The wavelength of the incident plane wave is 0.6328 μm. The incident plane wave is oscillated sinusoidally in the time domain, and the amplitude of the electric field is set to unity for simplicity.

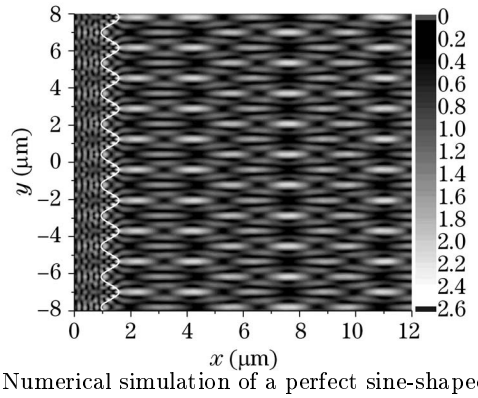

Fig. 1. Numerical simulation of a perfect sine-shaped grating with period of 2.6λ and the modulation depth of λ. The near-field distribution along with the increased distance. The Talbot images appear periodically in the x direction.

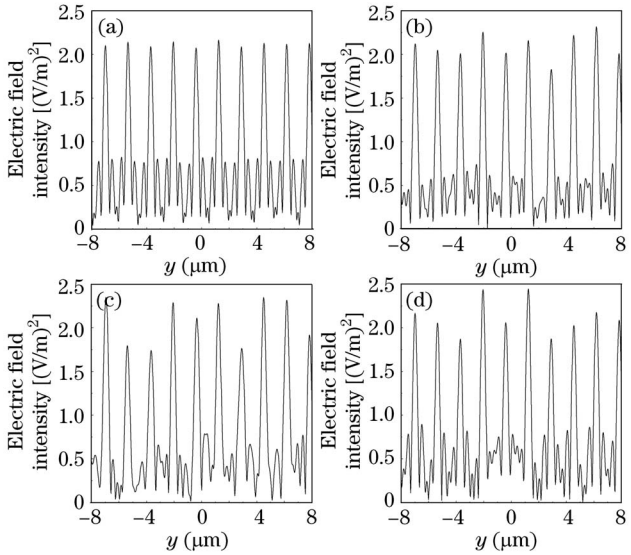

Fig. 2. the Distribution of the electric field intensity at 1/4 Talbot distances. (a) A perfect sine-shaped grating, (b) a distorted grating with a slight random magnitude fluctuation of $\lambda/10$, It is slightly different from the perfect Talbot imaging, (c) a distorted grating with a larger random magnitude variation of $\lambda/4$, which is obviously different from the perfect imaging in (a), (d) a grating with a half of the central period destroyed, which is different from (a). But it is hard to tell the difference between (c) and (d).

At first, we investigate a perfect sinusoidal grating with the parameters above. Figure 1 shows the numerical simulation of the electric field intensity distribution at different sample points. The Talbot images appear periodically in the x direction. The electric field intensity distribution at 2.6 μm (about 1/4 Talbot distance) away from the grating is shown in Fig. 2(a).

The FDTD method is a powerful method that can be used to analyze the diffraction in the near field with the distorted grating, which might be caused by the fabrication errors, such as the irregular flaws. We analyzed the Talbot effect with three different kinds of errors. The first is a slight fluctuation of the grooves in the grating, with a random magnitude variation of $\lambda/10$. It is slightly different from the perfect grating. The second is a distorted grating with a larger random variation of $\lambda/4$. The fault in these two cases is stochastic. The third is a grating with a half of the central period destroyed.

To see the influence of the flaws, the distribution of the electric field intensity at 1/4 Talbot distance is shown in Figs. 2(b), (c), and (d). For the first case, because the fluctuation in the grating is very slight, its influence is also small. The Talbot image at 1/4 Talbot distance as shown in Fig. 2(b), is not perfect as Fig. 2(a). There is a slight variation of the peak intensity in Fig. 2(b). For the second case, it is a distorted grating with a larger fluctuation. The influence of the flaw is very evident. The distribution of the electric-field intensity at 1/4 Talbot distance shows the influence of the flaw clearly. In comparison of the fluctuation of these two cases, it seems that the Talbot image looks like the profile of the original grating. The question is whether we can obtain the profile of a grating by detecting its Talbot image. In other words, can we obtain the profile of the flaws in a grating from the detected Talbot image? To answer this question, we study another case, a half of the central period of a grating is destroyed. The distribution of the electric field intensity at 1/4 Talbot distance is shown in Fig. 2(d). Similar to the former two cases, the Talbot image is also distorted, but the Talbot image does not resemble its original profile of the grating. In comparison of Fig. 2(c) and (d), we can see that the Talbot images are similar, but the original errors in the input gratings are quite different. That is to say, we cannot know the original profile of a grating by simply detecting its Talbot images. But we know that the grating would be perfect, if a perfect Talbot image is detected.

In conclusion, by using the rigorous FDTD electromagnetic computational model, we analyzed the Talbot effect with different kinds of faulty. This method requires long computing time and huge memory space. But for this irregular flaw, the FDTD method can show the exact near-field distribution, which is impossible to obtain with the conventional Fourier transform method. The results of the numerical simulations indicate that if the Talbot images of a grating are not perfect, the surface quality of the grating must be not good. From the Talbot images, we cannot obtain the detail of the flaws in the grating, because different kinds of flaws may result in similar noise in the Talbot images. If a grating is perfect, its Talbot imaging should also be perfect. For practical applications it is always necessary to use the perfect grating, not the distorted gratings. To this end, we do not care about the detailed information of a distorted grating. In this sense, we can evaluate a high-density grating according to its Talbot image. Smaller fluctuation of the detected Talbot image implies the better quality of the grating under test.

The authors acknowledge the support of the National Outstanding Youth Foundation of China (No. 60125512) and Shanghai Science and Technology Committee (No. 036105013, 03XD14005, 0359nm004). Y. Lu's e-mail address is yqlu@mail.siom.ac.cn.

References

1. W. H. F. Talbot, Philos. Mag. **9,** 401 (1836).
2. M. V. Berry and S. Klein, J. Mod. Opt. **43,** 2139 (1996).
3. C. Zhou, S. Stankovic, and T. Tschudi, Appl. Opt. **38,** 284 (1999).
4. C. Zhou, H. Wang, S. Zhao, P. Xi, and L. Liu, Appl.

Opt. **40,** 607 (2001).
5. C. Zhou, W. Wang, E. Dai, and L. Liu, Opt. Phot. News Dec **15,** 46 (2004).
6. K. S. Yee, IEEE Trans. Antenna Propag. **14,** 302 (1966).
7. A. Taflove and, S. Hagness, *Computational Electromagnetics: the Finite-Difference Time Domain Method* (2 edn.) (Artech House, Boston, 2000).
8. J. W. Wallance and M. A. Jensen, J. Opt. Soc. Am. A **19,** 610 (2002).
9. M. Qi, E. Lidorikis, P. T. Rakich, and S. G. Johnson, Nature **429,** 538 (2004).
10. P. Wei, H. Chou, and Y. Chen, Opt. Lett. **29,** 433 (2004).
11. H. Ichikawa, J. Opt. Soc. Am. A **15,** 152 (1998).
12. H. Ichikawa, J. Opt. Soc. Am. A **16,** 299 (1999).